Journal of Agricultural Engineering

https://www.agroengineering.org/

Design of a double-layer perforated air distribution system for greenhouses using computational fluid dynamics

Yerim Jo,[1] Sangik Lee,[2] Byung-hun Seo,[1] Jong-hyuk Lee,[3] Dongsu Kim,[1] Yejin Seo,[1] Dongwoo Kim,[1] Jimin Shim,[1] Won Choi[4]

[1]Department of Landscape Architecture and Rural Systems Engineering, College of Agriculture and Life Sciences, Seoul National University, Gwanak-gu, Seoul
[2]Department of Agricultural Civil Engineering, College of Agriculture and Life Sciences, Kyungpook National University, Buk-gu, Daegu
[3]Department of Landscape Architecture and Rural Systems Engineering, Research Institute of Agriculture and Life Sciences, College of Agriculture and Life Sciences, Seoul National University, Gwanak-gu, Seoul
[4]Department of Landscape Architecture and Rural Systems Engineering, Research Institute of Agriculture and Life Sciences, Integrated Major in Global Smart Farm, Greenbio Convergence and Open Sharing System, College of Agriculture and Life Sciences, Seoul National University, Gwanak-gu, Seoul, South Korea

Corresponding author: Won Choi, Department of Landscape Architecture and Rural Systems Engineering, Research Institute of Agriculture and Life Sciences, Integrated Major in Global Smart Farm, Greenbio Convergence and Open Sharing System, College of Agriculture and Life Sciences, Seoul National University, 1 Gwanak-ro, Gwanak-gu, Seoul, 08826, South Korea. E-mail: fembem@snu.ac.kr

Please cite this article as doi: 10.4081/jae.2025.1877

Submitted: 11 June 2025
Accepted: 10 October 2025

Design of a double-layer perforated air distribution system for greenhouses using computational fluid dynamics

Yerim Jo,[1] Sangik Lee,[2] Byung-hun Seo,[1] Jong-hyuk Lee,[3] Dongsu Kim,[1] Yejin Seo,[1] Dongwoo Kim,[1] Jimin Shim,[1] Won Choi[4]

[1]Department of Landscape Architecture and Rural Systems Engineering, College of Agriculture and Life Sciences, Seoul National University, Gwanak-gu, Seoul
[2]Department of Agricultural Civil Engineering, College of Agriculture and Life Sciences, Kyungpook National University, Buk-gu, Daegu
[3]Department of Landscape Architecture and Rural Systems Engineering, Research Institute of Agriculture and Life Sciences, College of Agriculture and Life Sciences, Seoul National University, Gwanak-gu, Seoul
[4]Department of Landscape Architecture and Rural Systems Engineering, Research Institute of Agriculture and Life Sciences, Integrated Major in Global Smart Farm, Greenbio Convergence and Open Sharing System, College of Agriculture and Life Sciences, Seoul National University, Gwanak-gu, Seoul, South Korea

Corresponding author: Won Choi, Department of Landscape Architecture and Rural Systems Engineering, Research Institute of Agriculture and Life Sciences, Integrated Major in Global Smart Farm, Greenbio Convergence and Open Sharing System, College of Agriculture and Life Sciences, Seoul National University, 1 Gwanak-ro, Gwanak-gu, Seoul, 08826, South Korea. E-mail: fembem@snu.ac.kr

Contributions: all the authors made a substantive intellectual contribution, read and approved the final version of the manuscript and agreed to be accountable for all aspects of the work.

Conflict of interest: the authors declare no competing interests, and all authors confirm accuracy.

Abstract
Single-layer perforated air ducts made of plastic films are widely used in greenhouses to control the root-zone environment of crops. However, conventional ducts often exhibit non-uniform airflow and thermal distributions along the duct length, making it difficult to maintain consistent environmental conditions in the greenhouse. To address this issue, a double-layer perforated air duct has been developed and implemented in greenhouses. However, it is necessary to quantitatively evaluate its effectiveness in improving environmental uniformity. In this study, computational fluid dynamics (CFD) simulations were conducted to compare the internal airflow and jet flow characteristics between the conventional single-layer duct and the proposed double-layer duct. In addition, three double-layer duct designs with different hole arrangements, sizes, and spacings were analyzed. The double-layer duct significantly improved the uniformity of the jet flow temperature and mass flow rate compared with the single-layer duct. The space between the inner and outer tubes in the double-layer duct acted as both a thermal insulation layer and a pressure chamber, maintaining a high, uniform internal static pressure and a low, consistent air velocity. The maximum improvement in temperature uniformity was 75%, and that in mass flow rate was 42%. The proposed double-layer perforated air duct can contribute to enhanced environmental uniformity in greenhouses by supplying jet flows through its holes at a more consistent temperature and mass flow rate along the duct length.

Key words: Computational fluid dynamics; indoor uniformity; greenhouse cultivation; perforated air duct; plastic film duct.

Introduction

Agricultural crop yields are being significantly affected by climate change and the corresponding inclement weather, and this trend is expected to continue. Climate change is associated with extreme weather events, such as floods and droughts, as well

as rising temperatures, and is forecasted to reduce crop yields and threaten food security (Bisbis *et al*., 2019; Goddek *et al*., 2023; Manzoor *et al*., 2024). To address these challenges and adapt to the growing threat posed by climate change, greenhouse cultivation has been proposed as an effective strategy, enabling stable crop production and improving agricultural productivity by protecting crops from external environmental stresses through environmental control (Gruda *et al*., 2019; Goddek *et al*., 2023). Stable crop yields can be achieved by maintaining appropriate temperature, humidity, and airflow conditions within the greenhouse. Owing to these advantages, the global area under greenhouse cultivation has been steadily increasing; by 2019, the world had seen approximately 1.3 million hectares of greenhouse infrastructure (Tong *et al*., 2024).

Various ventilation systems have been used to control the environment in greenhouses (Lee *et al*., 2019; Ghiasi *et al*., 2024), particularly of the root zone. The root zone plays a crucial role in water and nutrient absorption in crops and is highly sensitive to both high- and low-temperature stresses (Kwon *et al*., 2015; Llorach-Massana *et al*., 2017; Myung *et al*., 2024). Hence, perforated air duct systems have been widely adopted in greenhouses as environmental control methods for local heating and cooling strategies. Conventionally, single-layer plastic film air ducts have been employed to deliver conditioned air at an appropriate velocity and temperature through holes on the duct surface, which are placed beneath or between the crop canopies (Choi *et al*., 2015; Pardo-Pina *et al*., 2024).

However, conventional air duct systems often exhibit nonuniformity in terms of the supplied air temperature and flow along the duct due to heat loss through the duct surface and the pressure gradient along its length. Consequently, the air delivered to greenhouses will have a nonuniform temperature and velocity (Bailey, 1975; Kwon *et al*., 2015; Cao *et al*., 2023). Such environmental nonuniformity can lead to increased crop production costs because of the additional energy required to mitigate environmental variations and inconsistent crop growth (Baek *et al*., 2015). Hence, it is

necessary to develop strategies that enhance environmental uniformity, achieve stable crop production, and promote sustainable practices in agriculture (Lee *et al*., 2019; Lu *et al*., 2023).

The application of conventional ducts in greenhouses is associated with environmental variations given that the temperature and velocity of the delivered air exhibit nonuniformity. Hence, a double-layer perforated air duct has been developed to mitigate environmental variations between the upstream and downstream regions of a greenhouse. Unlike conventional single-layer ducts, double-layer ducts comprise an inner tube and an outer tube. Several studies have been conducted to improve the environmental uniformity of greenhouses using double-layer perforated air ducts. For example, Kim *et al*. (2004) developed a double-layer duct in which the area of the holes on the inner tube increased downstream, whereas the outer tube had a uniform hole size and spacing along its length. This design enables more amount of heated air to be supplied from the inner tube to the outer tube along the duct, thereby improving the thermal uniformity in the duct. Kim *et al*. (2004) found that variations in temperature and air velocity within a greenhouse decreased when using a double-layer duct; field experiments conducted in a single-span greenhouse revealed that this duct design could help enhance the growth of cucumbers. Kwon *et al*. (2015) developed a double-layer duct comprising an inner tube without holes and an outer tube with holes, whose spacing decreased downstream. They found that the temperature variation within the greenhouse could be minimized when the length of the inner tube was two-thirds that of the outer tube in a 90 m-long single-span greenhouse.

Previous field studies on double-layer ducts have primarily focused on the effect of duct design on improving temperature uniformity within greenhouses and enhancing crop growth. However, the internal airflow characteristics within the duct, characteristics of the jet flow through the holes, and effectiveness of the double-layer duct in delivering a uniform jet flow have been overlooked. For an effective application of double-layer ducts in greenhouses from the perspective of supplying air with uniform

temperature and flow rate, it is essential to understand the flow characteristics within the ducts. However, few experimental or theoretical studies have investigated these characteristics.

Several studies have investigated the airflow characteristics inside conventional plastic-film air ducts, characteristics of the jet flow through holes, and ventilation characteristics in greenhouses equipped with such ducts through field experiments (Teitel *et al*., 1999; Gladyszewska-Fiedoruk *et al*., 2011; Cámara-Zapata *et al*., 2020; Hekal *et al*., 2023). However, a strategy for evaluating the air velocity, pressure drop, and heat transfer within ducts through field experiments has not been clearly established. Moreover, field experiments are expensive (Mondaca and Choi, 2016; Cao *et al*., 2023).

Computational fluid dynamics (CFD) is a computational technique that approximates fluid flow solutions by discretizing and solving continuity, momentum, and energy equations using numerical methods. With the CFD technology, the time and cost associated with conducting actual field experiments can be saved, and the airflow characteristics and heat transfer inside perforated air ducts can be investigated. CFD studies have been performed on airflow and heat transfer inside conventional single-layer ducts (Mondaca and Choi, 2016; Farajpourlar, 2017; Raphe *et al*., 2021; Cao *et al*., 2022; Cao *et al*., 2023; Hekal *et al*., 2023). Hence, this study applied the CFD technique to evaluate the effectiveness of a double-layer perforated air duct on improving environmental uniformity inside greenhouses, followed by a comparison with the conventional single-layer air duct. The comparison between the single-layer and double-layer ducts, both made of plastic films, was made in terms of the airflow and temperature inside the duct as well as those of the jet flow. Moreover, three double-layer perforated air duct designs were analyzed, and the effects of hole arrangement, size, and spacing on the airflow and jet flow characteristics were evaluated.

Materials and Methods

Description of perforated air duct

Figure 1 shows a schematic of the perforated air duct system used in a greenhouse. The system comprises a heat exchanger module, including an axial fan and a heat exchanger; a connection module between the heat exchanger module and the duct; and the air duct itself. The proposed double-layer perforated air duct is composed of inner and outer tubes, with air supplied into the inner tube by an axial fan. Air in the inner tube is transferred to the outer tube through holes on the surface of the inner tube and discharged into the greenhouse through holes in the outer tube. The duct can be installed below crop canopy, supplying air of appropriate temperature and velocity to the root zone of the crops. With the double-layer duct delivering uniform airflow with consistent temperature and velocity, it becomes possible to maintain more uniform environmental conditions inside the greenhouse.

The target greenhouse is a Venlo-type glass greenhouse, with 20 continuous spans, a total length of 131.6 m, a side height of 5.9 m, and an edge height of 6.7 m. The width of each span is 4.0 m. Figure 1 shows the specifications of the greenhouse, along with the installed air duct system. The diameter of the outer tube of the duct was set to 650 mm, considering the side height of the greenhouse and growth height of the crop canopy. The inner tube diameter and the lengths of both the outer and inner tubes were set to 600 mm, and 126 m, respectively, considering the general specifications of double-layer ducts used in practice and allowing for sufficient workspace. In each of the two spans, five ducts were installed beneath the crop canopy as shown in Figure 1a.

Scenarios

The spacing, size, and arrangement of the holes on the duct surface affect the airflow pattern inside the duct and the jet flow characteristics (Raphe *et al*., 2021). Figure 2 shows the three double-layer perforated air ducts that were compared in this study to investigate the effect of hole configuration on the double-layer duct. Four

scenarios were considered. The first scenario (S1) was a double-layer duct in which both the inner and outer tubes had holes with a diameter of 20 mm and a spacing of 200 mm. Two holes were arranged at angles of 180° on the inner tube and 120° on the outer tube. The second scenario (S2) was a double-layer duct in which both the inner and outer tubes had holes with a diameter of 10 mm and a spacing of 110 mm. Four holes were arranged at an angle of 120° with respect to the inner tube, and two holes were arranged at an angle of 120° with respect to the outer tube. The third scenario (S3) had the same hole diameter on both the outer and inner tubes and the same spacing on the inner tube as S2, but it differed in that the hole spacing on the outer tube was 110 mm.

The first and second scenarios (S1 and S2) are typically applied in greenhouses. The third scenario (S3) was proposed to compare the flow patterns with varying area ratios of the holes between the inner tube (A_{IH}) and those on the outer tube (A_{OH}). The primary scenario (S0) was a conventional single-layer duct realized by removing the inner tube from S1. Table 1 lists the specifications for the four scenarios.

Computational fluid dynamics (CFD)

Geometry

Figure 3 shows the geometry of the ducts used in the CFD simulation. The total length of the ducts in S0 to S3 was modeled as 126 m, and a distance of 0.2 m between the axial fan and duct was considered to account for the connection module between the heat exchanger module and the duct. The geometry of the CFD simulation comprised four faces for the wall, one face for the inlet, and multiple faces for the outlet and interior walls (Hekal *et al.*, 2023). The solid surfaces of both the outer and inner tubes were set as walls, the holes on the inner tubes were set as "interior" boundary conditions to allow airflow through them, and the holes on the outer tubes were set as pressure outlets. Accordingly, the numbers of faces at the outlet were 1260, 1260, 4580, and 2290 for S0, S1, S2, and S3, respectively. The numbers of faces in the

interior were 1260, 4580, and 2290 for S1, S2, and S3, respectively.

Governing equation and solver setting

The Fluent R2 (Ansys, Inc., Canonsburg, PA, USA) was used to analyze the airflow and heat transfer inside the ducts and through holes. Ansys Fluent R2 is a CFD software based on the finite volume method and can be used to perform turbulence analyses by solving the Navier-Stokes equations. The general governing equations in Fluent R2 are the continuity, momentum, and energy equations, and they can be generalized using Eq. (1) (Patankar, 1980).

$$\nabla \cdot (\rho u \phi) = \nabla \cdot \left(\Gamma_\phi \nabla \phi\right) + S_\phi \qquad \text{(Eq. 1)}$$

where ρ is the density (kg·m^{-3}), u is the velocity (m·s^{-1}), ϕ is the dependent variable (velocity, temperature, and thermal conductivity), Γ_ϕ is the diffusion coefficient for ϕ, and S_ϕ is the source term for ϕ.

In this study, the realizable k–ε model was applied for the turbulence analysis, along with enhanced wall treatment. The realizable k–ε model has been widely used for analyzing airflow inside air ducts and has been validated for accurately predicting internal duct flow and jet flow from holes on ducts (Mondaca and Choi, 2016; Raphe *et al*., 2021). To ensure the accuracy of the enhanced wall treatment, the mean value of Y^+ was less than 5.

Boundary condition

The airflow was assumed to be steady and incompressible. The temperature outside the duct was set to 293.15 K at atmospheric pressure. The inlet of the duct, where air was supplied, was set as a mass flow inlet with a mass flow rate of 2.72 kg·s^{-1} and a temperature of 313.15 K. The holes on the duct surface were set as pressure outlets.

The fluid properties of the air were obtained from the Ansys Fluent R2 material database. The properties of the duct surface were obtained from Zhang *et al*. (2021), including a density of 915 kg·m^{-3}, heat capacity of 1,900 J·kg^{-1} K^{-1}, and thermal

conductivity 0.33 $W \cdot m^{-1} K^{-1}$.

Grid independence test

Mesh quality affects both the accuracy and stability of CFD simulations. A finer mesh improves the accuracy and convergence of the simulation but results in a higher computational cost. In this study, the mesh was generated using tetrahedral elements. Inflation layers were created with finer mesh elements near the duct walls and around the holes. Table 2 lists the number of elements and minimum element size for the coarse, normal, and fine meshes across S0 to S3. Figure 4 shows the fine mesh generated for S1.

Grid independence tests were conducted for each scenario from S0 to S3, comparing the coarse, normal, and fine meshes. To conduct the test, the mass flow rate and temperature of the jet flow through the holes on the outer tube were compared across the three meshes. Figure 5 shows the results of the grid-independence test for S1. The relative differences in the average mass flow rate of the jet flow between the coarse and normal grids were approximately 0.7% (S0), 4.1% (S1), 3.4% (S2), and 4.8% (S3). The relative differences in the temperature of the jet flow between the coarse and normal grids were approximately 0.1% (S0), 0.9% (S1), 1.1% (S2), and 1.0% (S3). The relative differences in the average mass flow rate of the jet flow between the normal and fine grids were approximately 1.6% (S1), 0.7% (S2), and 4.1% (S3). The relative differences in the temperature of the jet flow between the normal and fine grids were approximately 0.2% (S1), 0.1% (S2), and 0.2% (S3). To ensure a higher accuracy of the analysis, a fine mesh was selected based on the grid independence test results.

CFD model validation and statistical assessment

To validate the proposed CFD model, a field experiment was conducted in the target greenhouse to measure the velocity of jet flow from the holes of S3. The air velocity of jet flow in S3 was measured at intervals of 30 m along the duct, using a portable hot wire anemometer (Testo 435-4 Multifunction indoor air quality meter,

Testo, Germany). The measurement range of the hot wire anemometer was 0 - 20 $m \cdot s^{-1}$, with an accuracy of ± 0.01 $m \cdot s^{-1}$.

Analysis of variance (ANOVA) at a significance level of 0.05 was used to assess whether the differences between the experimental and simulation results were statistically significant, and to evaluate whether the differences between the three double-layer duct designs (S1 to S3) in the CFD simulation results were statistically significant. The mean absolute percentage error (MAPE) was used to calculate the average percentage error between the experimental and simulation results.

$$\text{MAPE} = \frac{1}{n}\sum_{i=1}^{n}\left|\frac{y_{i,exp}-y_i}{y_{i,exp}}\right| \times 100\ (\%) \qquad \text{(Eq. 2)}$$

where n is number of data points, $y_{i,exp}$ is the *i*th experimental value, and y_i is the *i*th predicted value.

Results and Discussion

CFD model validation

Figure 6 shows the experimental and simulation values of the velocity of jet flow at intervals of 30 m along S3 duct. The relative errors between experimental and simulation values ranged from 2.9% to 12.0%, resulting in a MAPE of 5.2%. Based on ANOVA, the p-value (0.19) was greater than the significance level (0.05), indicating that there was no statistically significant difference between the experimental and simulation values. The overall trend in the velocity variation was also consistent. This confirms the validity of the proposed CFD model in investigating the airflow characteristics of perforated air ducts.

Effect of inner duct wall on jet flow

Mass flow rate of jet flow

The uniformity of the airflow in greenhouses affects the temperature, humidity, and CO_2 distributions, which, in turn, influence crop growth (Fernandez and Bailey, 1994; Li *et al*., 2024). To evaluate the effectiveness of a double-layer duct in improving environmental uniformity inside greenhouses, the mass flow rate of the jet flowing through the holes on the outer tube was compared between S0 and S1, which correspond to single- and double-layer ducts, respectively, with identical hole arrangements, sizes, and spacings. Based on ANOVA, the p-values for the mass flow rate, velocity, and temperature of jet flow between S0 and S1 were all less than 0.001, which is below the significance level of 0.05. This indicates that the differences in the simulation results between S0 and S1 are statistically significant. Figure 7 a,b shows the mass flow rate and velocity of the jet flows, respectively, along the duct length at intervals of 5 m for both S0 and S1. The results showed that the mass flow rate of the jet increased when the hole was far from the axial fan in both scenarios. The difference in the mass flow rate between the hole closest to the fan and the hole farthest from the fan was 5.3 $kg{\cdot}h^{-1}$ in S0 and 2.3 $kg{\cdot}h^{-1}$ in S1. Thus, the mass flow rate of the jet flow was more uniformly distributed in S1 than in S0.

These results are consistent with previous results. Chen and Sparrow (2009) and Farajpourlar (2017) measured the mass flow rates of the jet flow from the holes of a manifold and confirmed that the mass flow rate of the jet flows from holes located farther from the inlet was higher than that from those located closer to the inlet. Hekal *et al*. (2023) conducted experiments on perforated fabric air ducts and measured the static pressure inside the ducts. They observed that the static pressure inside the duct increased along the duct length. Similarly, Farajpourlar (2017) and Cao *et al*. (2023) simulated the increase in the rate of mass flow through holes along the length of a manifold and fabric air ducts using the CFD technique and validated the accuracy of the simulation model by comparing the experimental and simulation results. This phenomenon can be attributed to the static regain effect within the perforated ducts. The mass flow rate of a jet flow primarily depends on the static pressure difference across the holes (Bailey, 1975; Farajpourlar, 2017; Tadj *et al*., 2017). The static regain effect is the increase in the static pressure inside a perforated air duct along its length. This is because air discharge from the holes in the duct decreases the mass flow rate inside the duct. This reduction in the mass flow results in a decrease in the dynamic pressure inside the duct, and the static pressure correspondingly increases by the same amount as the decrease in the dynamic pressure (Bailey, 1975). Consequently, the static pressure difference across the holes increased in the downstream direction, resulting in an increase in the mass flow rate of the jet flowing along the duct.

Figure 8 shows the static pressure and velocity near the outer tube surfaces for S0 and S1. In S1, the air velocity near the wall was not only lower but also more uniform along the duct length than in S0. This phenomenon can be attributed to the presence of a pressure chamber between the inner and outer tubes in the double-layer duct, where air is discharged from the holes in the inner tube into a relatively large space. In S0, the static pressure continuously increased, and the velocity continuously decreased near the outer tube surface downstream. In contrast to S0, in S1, the air velocity near the outer tube surface remained low and uniform, below 2 $m \cdot s^{-1}$, although the static

pressure also increased downstream. According to previous studies, Kim and Lee (2017) and Jang *et al*. (2021) found that when air was injected from a narrow space into a wider space, the space in between could act as a pressure chamber. The pressure chamber minimizes pressure loss and maintains uniform pressure (Kim and Lee, 2017). Consequently, the mass flow rate of the jet flow in S1, which corresponds to the double-layer duct, was more uniform than that in S0 owing to the formation of a pressure chamber near the outer tube surface.

Jet flow temperature

When the temperature inside a duct is higher than that outside, convective heat transfer occurs on the duct surface, resulting in a decrease in the internal duct temperature in the downstream direction. This phenomenon leads to a decrease in the temperature of the air injected from the duct along the duct length, thereby leading to temperature variations within the greenhouse (Kwon *et al*., 2015). To evaluate the effectiveness of a double-layer duct in improving environmental uniformity, the temperature of the jet flowing through the holes on the outer tube was compared between S0 and S1, which correspond to single-layer and double-layer ducts, respectively. Figure 7c shows the temperature of the jet flowing along the duct length at intervals of 5 m in both S0 and S1. The results showed that the temperature of the jet flow decreased when the hole was far from the axial fan in both scenarios. The temperature difference between the hole closest to the fan and that farthest from the fan was 16 K in S0 and 6 K in S1. Thus, it can be confirmed that the jet flow temperature was more uniformly distributed in S1 than in S0.

In a previous study conducted by Kim *et al*. (2004), the temperature difference between the upstream and downstream of a 90 m-long single-span greenhouse was 15 K when a conventional single-layer duct was installed, whereas it was reduced to 1 K when they installed their double-layer duct. Furthermore, the installation of the double-layer duct led to a 15% increase in the average weight of cucumbers owing to the improved thermal uniformity.

Figure 9a shows the cross-sectional distributions of the temperature inside the ducts for S0 and S1. For both S0 and S1, the temperature decreased downstream, as shown in Figure 9a. Figure 9b shows the temperature near the outer tube surface and at the center of the cross section for both S0 and S1. This phenomenon is attributed to the presence of an air gap, which is the space between the inner and outer tubes of a double-layer duct. This air gap acts as a thermal insulation layer in the double-layer duct (Bruno *et al*., 2021). Although the average heat transfer coefficients on the outer tube surface were similar between S0 and S1, evaluated to be 25.0 and 25.6 $W \cdot m^{-2} \cdot K^{-1}$, respectively, the heat transfer coefficient on the inner tube surface in S1 was significantly lower at 2.1 $W \cdot m^{-2} \cdot K^{-1}$. Consequently, the temperature inside the inner tube of S1 was relatively uniform. In S1, the heat transfer from the inner tube to the space between the inner and outer tubes was substantially reduced. Consequently, the temperature near the outer tube surface in S1 was lower than that in S0, up to approximately 40 m downstream from the axial fan, resulting in a lower temperature of the air injected through the holes on the outer tube in S1 compared with S0. However, beyond 40 m downstream, the temperature near the outer tube in S1 was higher than that in S0 because warmer air inside the inner tube continued to be supplied to the space between the inner and outer tubes. This led to a more uniform and higher temperature of the jet flows in S1 than in S0, as shown in Figure 9, which shows the longitudinal temperature distribution along the duct.

Effect of hole design on double-layer duct

The effects of hole arrangement, size, and spacing on the environmental uniformity in the greenhouse were evaluated by comparing the three double-layer duct designs. Based on ANOVA, the p-values for the mass flow rate, velocity, and temperature of jet flow between the three double-layer duct designs (S1 to S3) were all less than 0.001, which is below the significance level of 0.05. This indicates that the differences in their simulation results are statistically significant.

To compare the rates of mass flow through the holes in the ducts of different sizes and arrangements, the mass flow rate at each hole was normalized using the average mass flow rate within each double-layer duct (S1 to S3). Figure 10 a,b shows the normalized mass flow rate and velocity of the jet flows, respectively, along the duct length at intervals of 5 m for S1 to S3. The results showed that both the mass flow rate and velocity of the jet flow increased when the hole was far from the axial fan in both scenarios. The velocity varied depending on the hole design parameters such as the hole diameter and the ratio of A_{OH} to A_{IH}, which differed between the three double-layer duct designs. The difference in the normalized mass flow rate between the hole closest to the fan and the hole farthest from the fan was 0.29 in S1, 0.29 in S2, and 0.14 in S3. Thus, the mass flow rate of the jet flow was uniformly distributed in S3. Figure 10c shows the temperature of the jet flowing along the duct length at intervals of 5 m for S1 to S3. The results indicated that the temperature of the jet flow decreased when the hole was far from the axial fan in both scenarios. The differences in temperature between the hole closest to the fan and the hole farthest from the fan were 6, 6, and 7 K in S1, S2, and S3, respectively. The heat transfer coefficients on the inner tube surface were 2.1, 2.7, and 2.7 $W \cdot m^{-2} \cdot K^{-1}$ in S1, S2, and S3, respectively.

The improvement in the environmental uniformity of the double-layer ducts was evaluated by comparing the coefficients of variation (CV) of the mass flow rate and temperature around the holes in the outer tube. Table 3 presents the CV values for the four scenarios, S0 to S3. The results showed that while the CVs for the temperature were similar among the double-layer duct designs (S1 to S3), ranging from 0.3% to 0.4%, the CVs for the mass flow rate varied significantly depending on the hole design of the double-layer duct. Compared with S0, the temperature uniformity improved by more than 65% in all the three double-layer duct designs. For the uniformity of the mass flow rate, the improvements compared with S0 were 11% in S1, 5% in S2, and 42% in S3. Therefore, S3 exhibited a notably greater uniformity in the mass flow rate than the other double-layer duct designs.

This difference can be attributed to the variation in the static pressure distribution within the ducts, which is influenced by the ratio of A_{OH} to A_{IH}. To compare the uniformity of the static pressure near the outer tube surface with different sizes and arrangements, the static pressure was normalized by the average value within each double-layer duct (S1 to S3). Figure 11 shows the normalized static pressure near the outer tube surface along the duct length at intervals of 5 m for S1 to S3. In S3, the static pressure near the outer tube surface is the most uniform among the three designs. In conclusion, although the temperature uniformity of the jet flows was similar across S1–S3, the mass flow rate uniformity of the jet flows varied significantly, demonstrating the most uniform distribution.

Conclusions

A double-layer perforated air duct is considered an effective ventilation system for improving environmental uniformity in greenhouses because it supplies jet flow with a more consistent temperature and mass flow rate along the duct length. In this study, CFD simulations were conducted to analyze the internal airflow and jet flow characteristics of double-layer ducts and to compare the effects of various hole configurations. The following conclusions are drawn from the CFD simulation results:

(1) In the double-layer duct (S1), the uniformity in the mass flow rate improved by 11% compared with the single-layer duct (S0). This improvement was attributed to the space between the inner and outer tubes in S1, which acted as a pressure chamber maintaining a high and uniform internal static pressure and a low and stable air velocity.

(2) In S1, the temperature uniformity improved by 75% compared with S0. This improvement was attributed to the thermal-insulation effect of the air gap, which is the space between the inner and outer tubes in S1. Consequently, the average heat transfer coefficient on the inner tube surface was as low as 2.1 $W \cdot m^{-2} \cdot K^{-1}$.

(3) Among the three designs of double-layer ducts, S3 with an A_{OH}-to-A_{IH} ratio of 0.5 showed the greatest improvement in the mass flow rate uniformity, of up to 42%, while temperature uniformity improved by over 65% across all designs. In all cases, the heat transfer coefficients were below 2.7 $W \cdot m^{-2} \cdot K^{-1}$. The superior performance of S3 was linked to its highest and most uniform internal static pressure.

In summary, our CFD simulations helped confirm that the double-layer duct design can improve the uniformity in the jet flow temperature and mass flow rate by up to 42% and 75%, respectively. The enhanced uniformity in the jet flow through the holes of the double-layer duct may help mitigate environmental nonuniformity inside greenhouses. In the future, for the application of double-layer ducts in greenhouses, it will be necessary to analyze the airflow characteristics inside greenhouses where double-layer ducts are installed and to validate the simulation results through real-world experiments. In particular, differences in velocity and temperature between the upstream and downstream of greenhouses should be evaluated to verify the effectiveness of double-layer ducts in improving environmental uniformity. Furthermore, crop growth performance in greenhouses equipped with single- and double-layer ducts should be compared to assess the benefits of the improved environmental uniformity.

Acknowledgements: This work was supported by the Korea Institute of Planning and Evaluation for Technology in Food, Agriculture, and Forestry (IPET) and the Korea Smart Farm R&D Foundation (KosFarm) through the Smart Farm Innovation Technology Development Program, funded by the Ministry of Agriculture, Food, and Rural Affairs (MAFRA), Ministry of Science and ICT (MSIT), and Rural Development Administration (RDA) (RS-2024-00402065).

References

Baek, M.S., Kwon, S.Y., Lim, J.H. 2015. Improvement of uniformity in cultivation environment and crop growth rate by hybrid control of air flow devices. J. Central South Univ. 22:4702–4708.

Bailey, B.J. 1975. Fluid flow in perforated pipes. J. Mech. Eng. Sci. 17:338–347.

Bisbis, M.B., Gruda, N.S., Blanke, M.M. 2019. Securing horticulture in a changing climate—A mini review. Horticulturae 5:56.

Bruno, R., Bevilacqua, P., Ferraro, V., Arcuri, N. 2021. Reflective thermal insulation in non-ventilated air-gaps: Experimental and theoretical evaluations on the global heat transfer coefficient. Energy Build. 236:110769.

Cámara-Zapata, J.M., Sánchez-Molina, J.A., Wang, H., Carreño-Ortega, A., Rodríguez, F. 2020. Evaluation of an adapted greenhouse cooling system with pre-chamber and inflatable air ducts for semi-arid regions in warm conditions. Agronomy 10:752.

Cao, M., Rong, L., Choi, C.Y., Wang, K., Wang, X. 2022. Computational evaluation of air jet cooling from a perforated air duct system to mitigate heat stress of cows in free stalls. Comput. Electr. Agric. 199:107198.

Cao, M., Yang, R., Choi, C.Y., Rong, L., Zhang, G., Wang, K., Wang, X. 2023. Effects of discharge angle of jet from a slot orifice on cooling performance for a perforated air duct system in dairy cattle barn. Comput. Electr. Agric. 210:107890.

Chen, A., Sparrow, E.M. 2009. Turbulence modeling for flow in a distribution manifold. Int. J. Heat Mass Transfr. 52:1573–1581.

Choi, K.Y., Jang, E.J., Rhee, H.C., Yeo, K.H., Choi, E.Y., Kim, I.S., Lee, Y.B. 2015. [Effect of root zone cooling using the air duct on temperatures and growth of paprika during hot temperature period].[Article in Korean with English abstract]. J. Bio-Environment Con. 24:243-251.

Kim, Y.J., Chung, S.O., Park, S.J., Choi, C.H. 2011. [Analysis of the power requirements of agricultural tractors by major field operation].[Article in Korean with English abstract]. J. Biosyst. Eng. 36:79–88.

Farajpourlar, M. 2017. On the prediction of uniformity of air flow out from manifold distribution. Mat-wiss. u. Werkstofftech. 48:249-254.

Fernandez, J.E., Bailey, B.J. 1994. The influence of fans on environmental conditions in greenhouses. J. Agric. Eng. Res. 58:201-210.

Ghiasi, M., Wang, Z., Mehrandezh, M., Paranjape, R. 2024. A systematic review of optimal and practical methods in design, construction, control, energy management and operation of smart greenhouses. IEEE Access 12:2830-2853.

Gladyszewska-Fiedoruk, K., Demianiuk, A.B., Gajewski, A., Olow, A. 2011. Measurement of velocity distribution for air flow through perforated plastic foil ducts. Energy Build. 43:374–378.

Goddek, S., Körner, O., Keesman, K.J., Tester, M.A., Lefers, R., Fleskens, L., et al. 2023. How greenhouse horticulture in arid regions can contribute to climate-resilient and sustainable food security. Glob. Food Secur. 38:100701.

Gruda, N., Bisbis, M., Tanny, J. 2019. Influence of climate change on protected cultivation: Impacts and sustainable adaptation strategies-A review. J. Clean Prod. 225:481–495.

Hekal, M., El-Maghlany, W.M., Eldrainy, Y.A., El-Adawy, M. 2023. Hydro-thermal performance of fabric air duct (FAD): Experimental and CFD simulation assessments. Case Stud. Therm. Eng. 47:103107.

Kim, J.Y., Lee, S.G. 2017. Study on design of pressure chamber in a linear-jet type air curtain system for prevention of smoke spread. Open J. Fluid Dyn. 7:501–510.

Kim, T.Y., Woo, Y.H., Mun, B.H., Kim, K.D., Cho, I.H., Nam, E.Y., Nam, Y.I. 2004. [Improving the distribution of temperature by a double air duct in the air-heated plastic greenhouse].[Article in Korean with English abstract]. J. Bio-Environ. Contr. 13:162-166

Kwon, J.K., Kang, G.C., Moon, J.P., Lee, T.S., Lee, S.J. 2015. [Effect of growing part following local heating for cherry tomato on temperature distribution of crop and fuel consumption].[Article in Korean with English abstract]. J. Bio-Environ. Contr. 24:217–225

Li, H., Lu, J., He, X., Zong, C., Song, W., Zhao, S. 2024. Effect of installation factors on the environment uniformity of multifunctional fan-coil unit system in Chinese solar greenhouse. Case Stud. Thermal Eng. 60:104818.

Llorach-Massana, P., Peña, J., Rieradevall, J., Montero, J.I. 2017. Analysis of the technical, environmental and economic potential of phase change materials (PCM) for root zone heating in Mediterranean greenhouses. Renew. Energy 103:570–581.

Lu, J., Li, H., He, X., Zong, C., Song, W., Zhao, S. 2023. CFD simulation and uniformity optimization of the airflow field in Chinese solar greenhouses using the multifunctional fan–coil unit system. Agronomy 13:197.

Manzoor, M.A., Xu, Y., Lv, Z., Xu, J., Shah, I.H., Sabir, I.A., et al. 2024. Horticulture crop under pressure: Unraveling the impact of climate change on nutrition and fruit cracking. J. Environ. Manage. 357:120759.

Mondaca, M.R., Choi, C.Y. 2016. A computational fluid dynamics model of a perforated polyethylene tube ventilation system for dairy operations. T. ASABE 59:1585–1594.

Myung, J., Cui, M., Lee, B., Lee, H., Shin, J., Chun, C. 2024. Development of a root-zone temperature control system using air-source heat pump and its impact on the growth and yield of paprika. AoB Plants 16:plae047.

Pardo-Pina, S., Ferrández-Pastor, J., Rodríguez, F., Cámara-Zapata, J.M. 2024. Analysis of an evaporative cooling pad connected to an air distribution system of perforated polyethylene tubes in a greenhouse. Agronomy 14:1187.

Patankar, S., 1980. Numerical heat transfer and fluid flow. 1st ed. Boca Raton, CRC Press.

Raphe, P., Fellouah, H., Poncet, S., Ameur, M. 2021. Ventilation effectiveness of uniform and non-uniform perforated duct diffusers at office room. Build. Environ. 204:108118.

Tadj, N., Nahal, M.A., Draoui, B., Constantinos, K. 2017. CFD simulation of heating greenhouse using a perforated polyethylene ducts. Int. J. Eng. Syst. Model. Simul. 9:3–11.

Teitel, M., Segal, I., Shklyar, A., Barak, M. 1999. A comparison between pipe and air heating methods for greenhouses. J. Agric. Eng. Res. 72:259–273.

Tong, X., Zhang, X., Fensholt, R., Jensen, P.R.D., Li, S., Larsen, M.N., et al. 2024. Global area boom for greenhouse cultivation revealed by satellite mapping. Nature Food *5*:513–523.

Zhang, W., Li, A., Zhou, M., Gao, R., Yin, Y. 2021. Flow characteristics and structural parametric optimisation design of rectangular plenum chambers for HVAC systems. Energy Build. 246:111112.

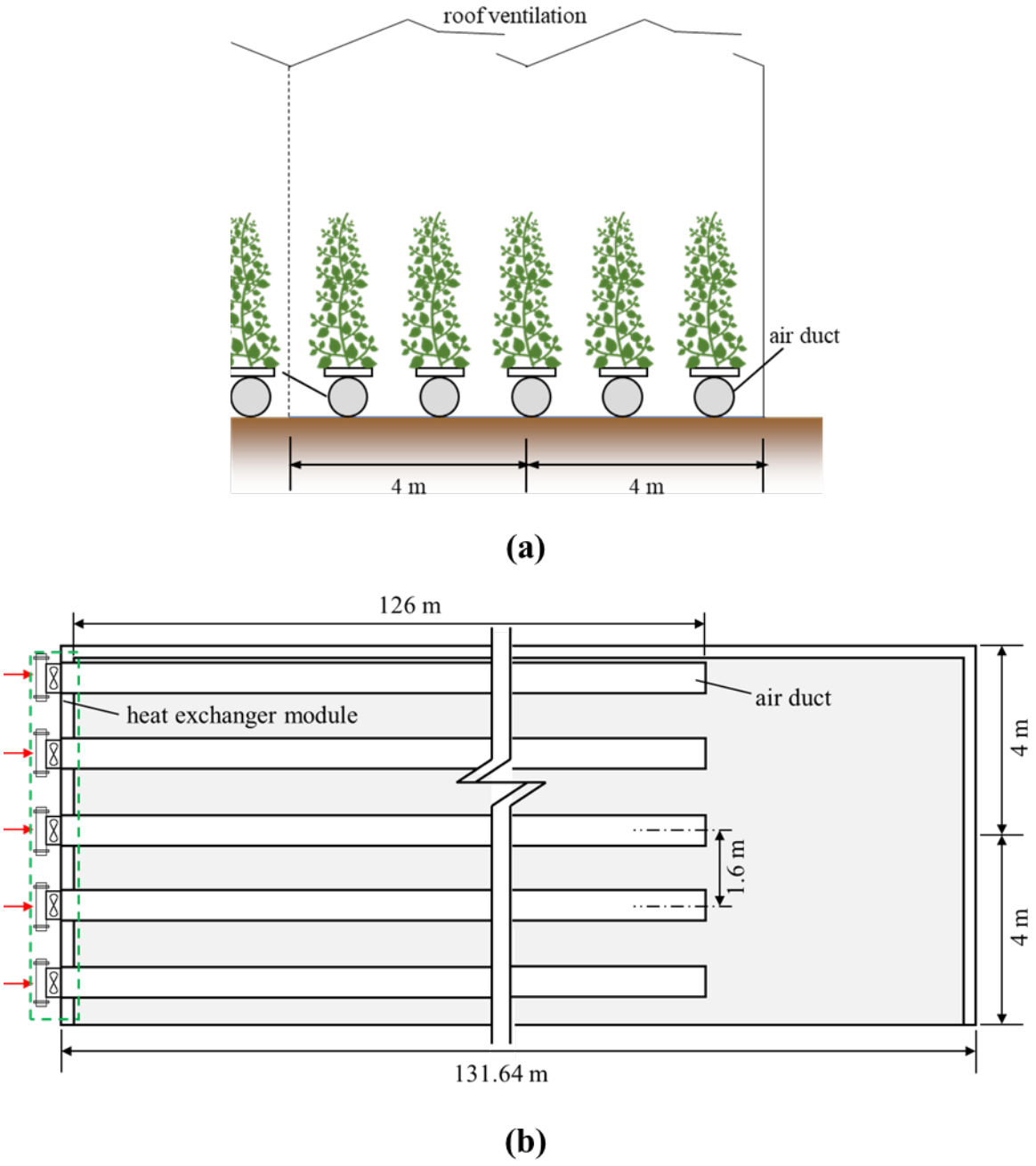

Figure 1. Schematic of the air duct system (a) front view (b) plan view.

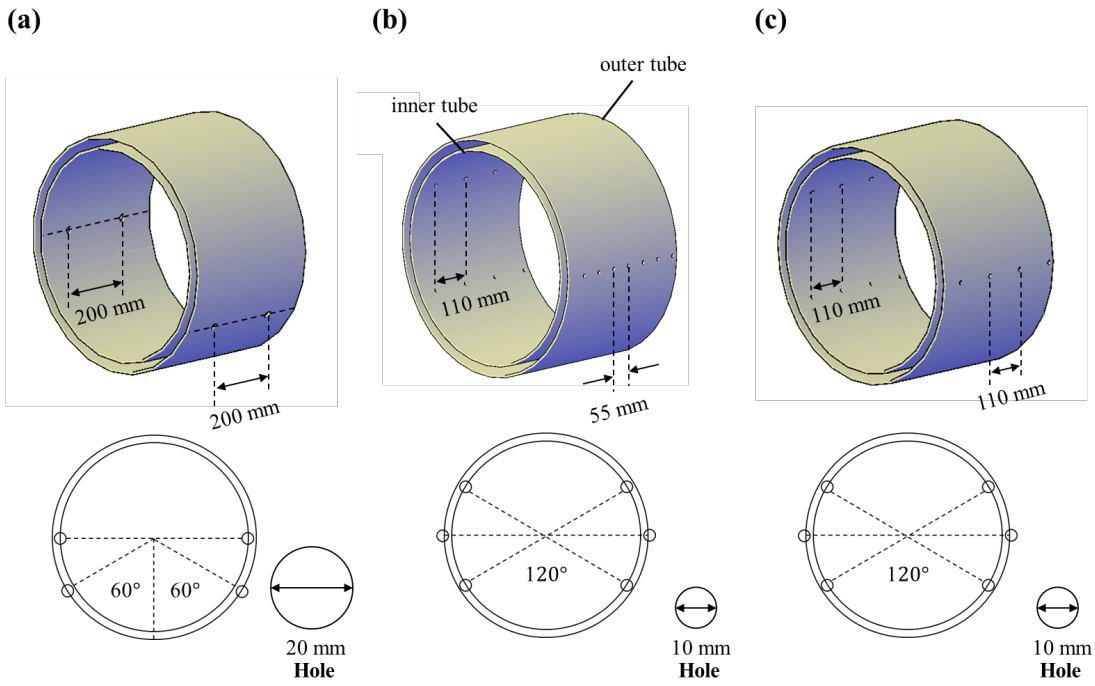

Figure 2. Three-dimensional views of a double-layer air duct: (a) S1, (b) S2, and (c) S3.

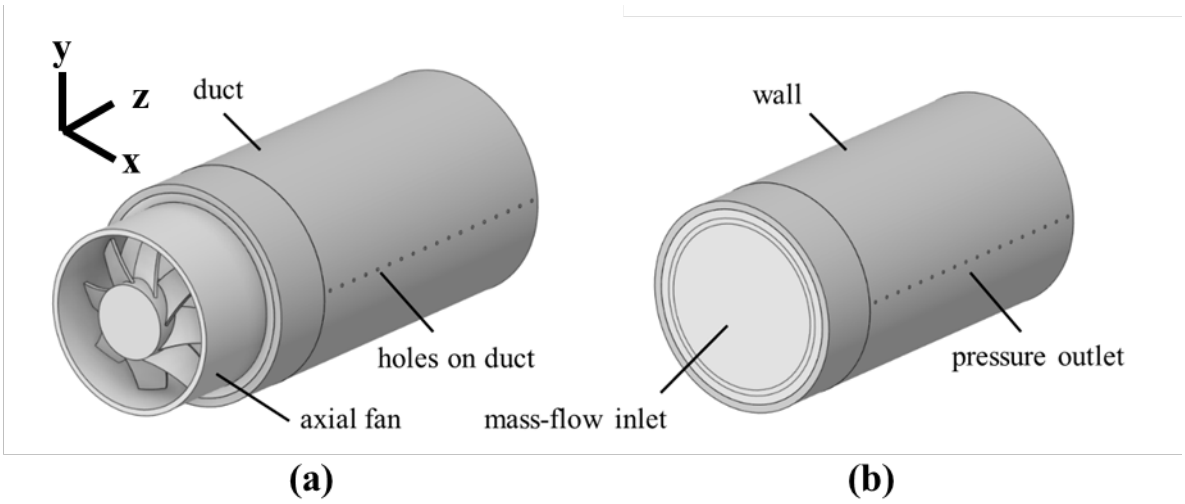

Figure 3. Geometry of air duct (a) actual structure (b) simplified model for CFD simulation.

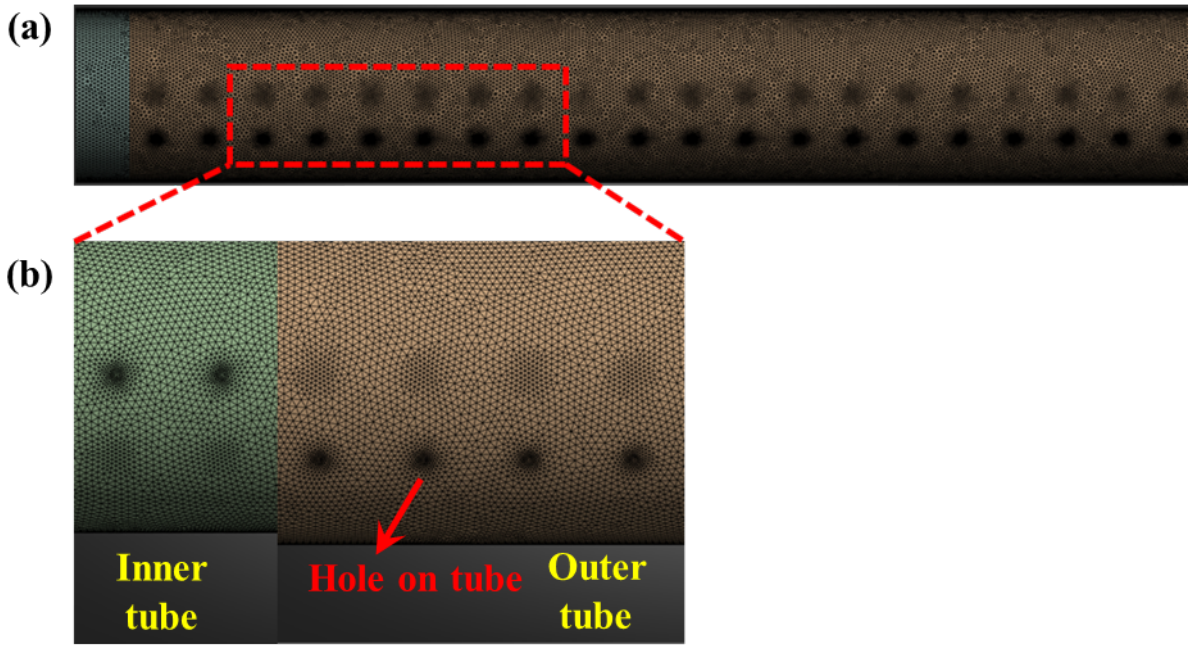

Figure 4. Generated fine mesh of S3 (a) side view (b) details of mesh.

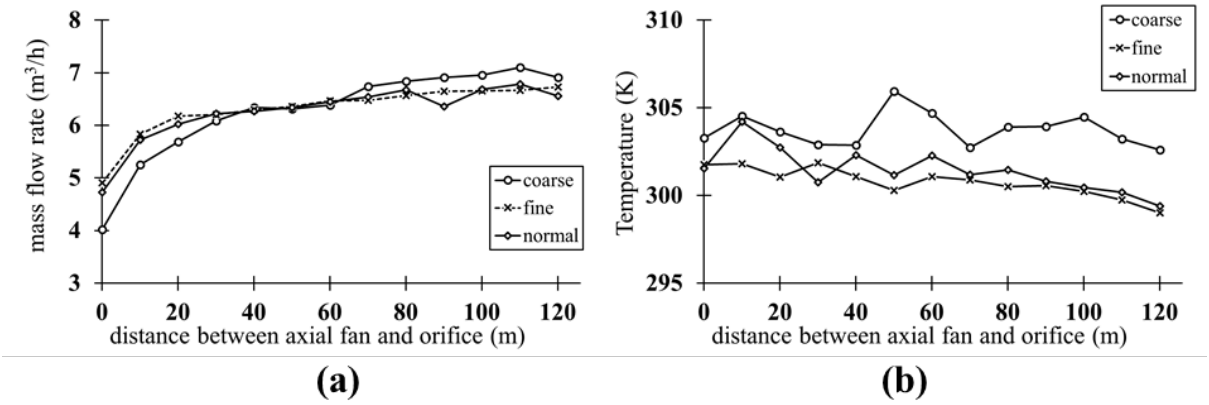

Figure 5. Grid independence test of S1: (a) mass flow rate of jet flow through outer tube holes, (b) temperature of jet flow through outer tube holes.

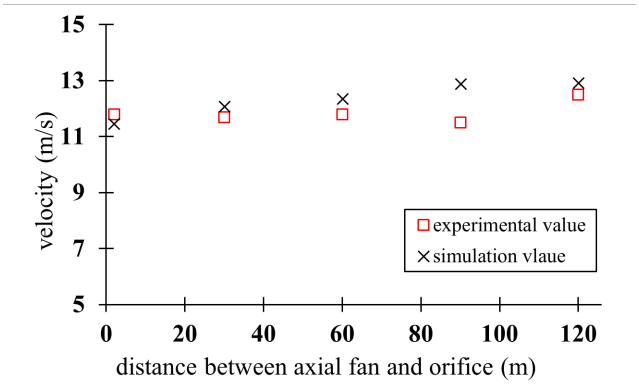

Figure 6 . Comparison between experimental value and simulation value in S3 based on velocity of jet flow.

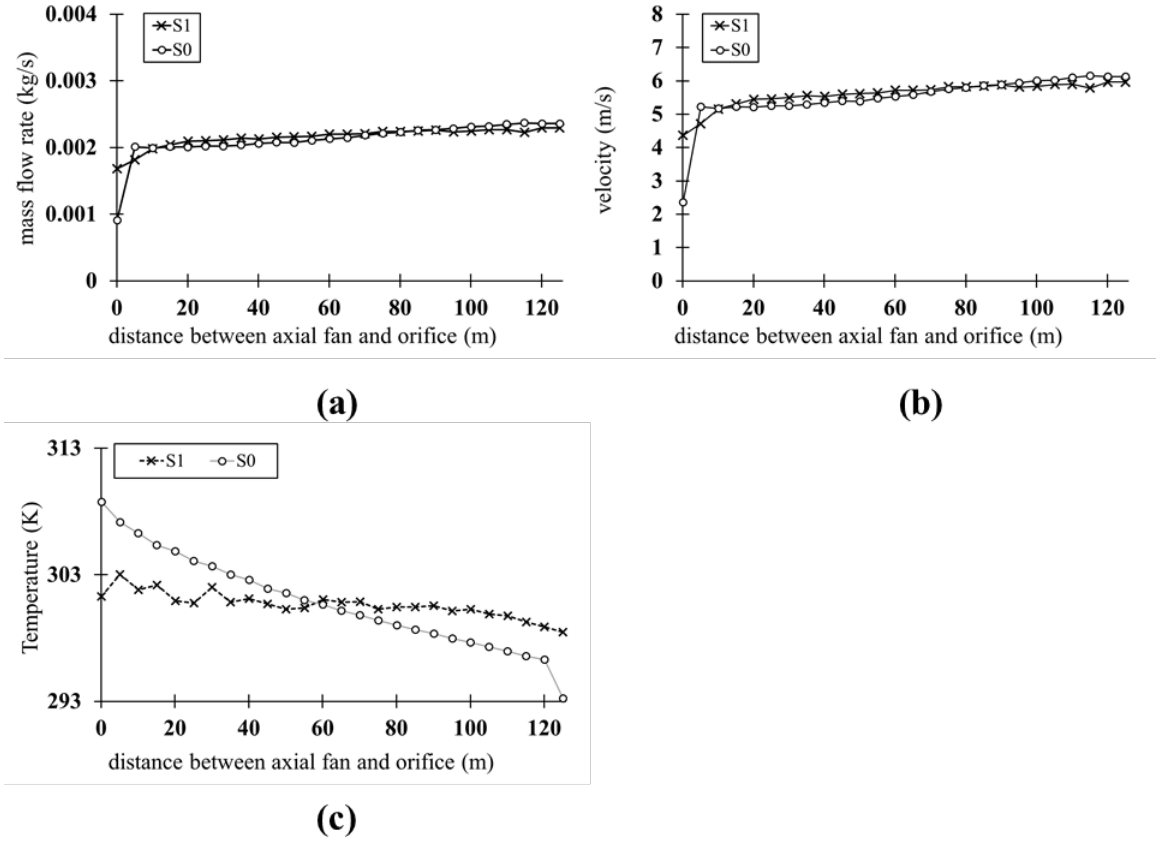

Figure 7. Comparison between single- (S0) and double-layer (S1) air ducts in terms of (a) mass flow rate of jet flow through outer tube holes, (b) velocity of jet flow through outer holes, (c) temperature of jet flow through outer tube holes.

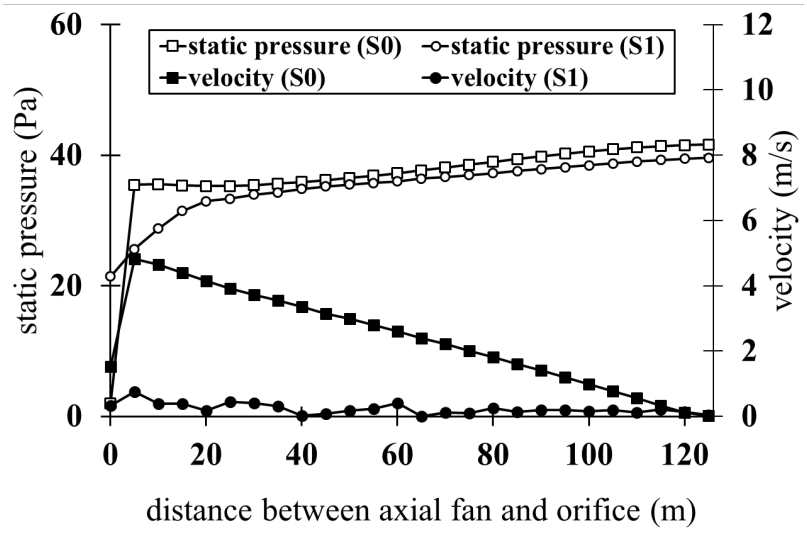

Figure 8. Comparison between single- (S0) and double-layer (S1) air ducts based on static pressure and velocity in the near-wall region.

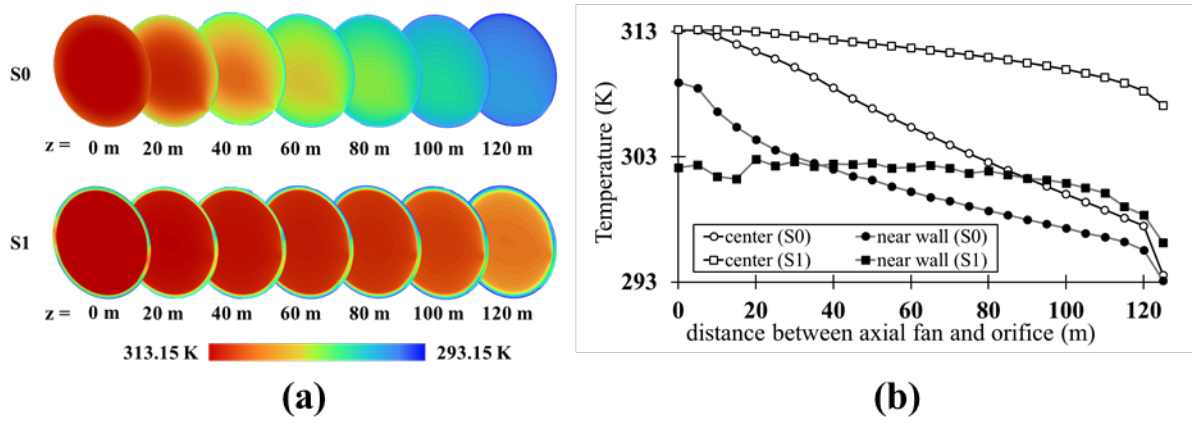

Figure 9. Comparison between single- (S0) and double (S1) air ducts based on temperature (a) Longitudinal temperature distribution inside the duct (b) temperature in the near-wall region and center of the section.

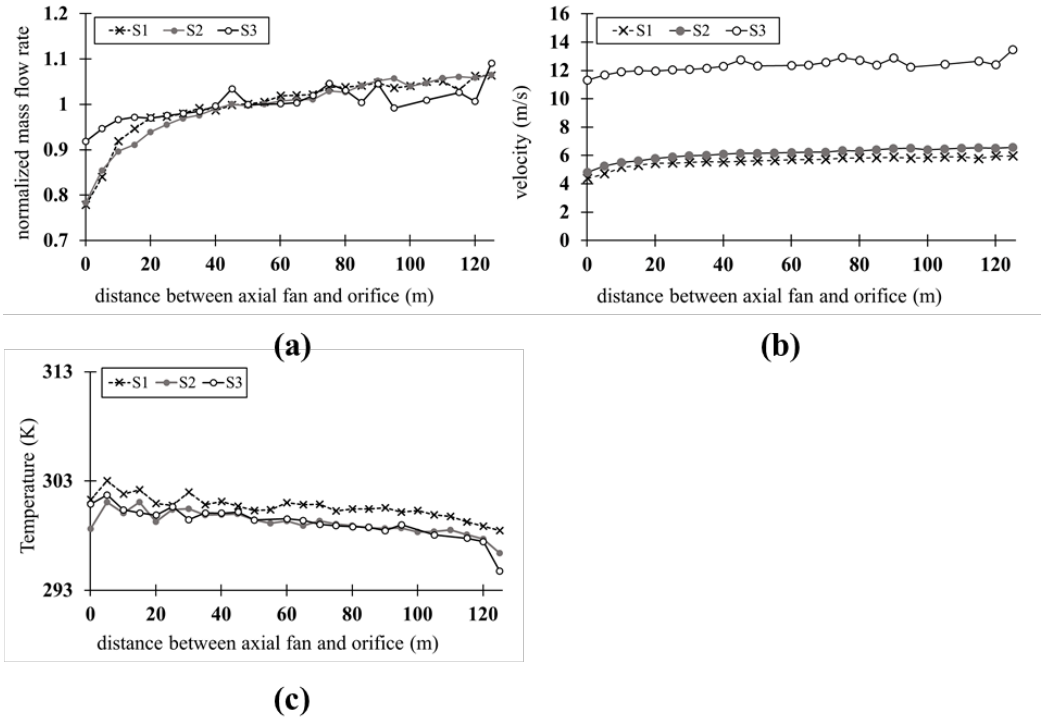

Figure 10. Comparison between three double-layer air ducts (a) mass flow rate of jet flow through outer tube holes, (b) velocity of jet flow through outer tube holes, (c) temperature of jet flow through outer tube holes.

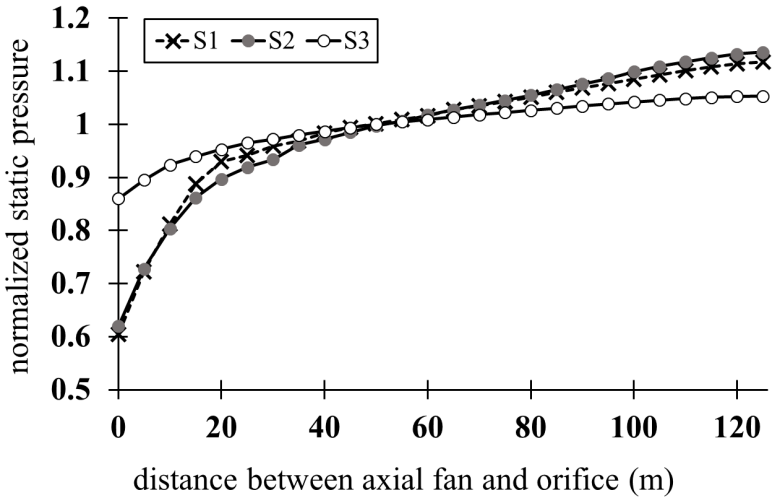

Figure 11. Comparison between three double-layer air ducts by static pressure in the duct.

Table 1. Description of scenarios for a perforated double-layer air duct.

Scenario		S0	S1	S2	S3
External duct	Type	Single layer		Double layer	
	Diameter (mm)	650	650	650	650
	Hole diameter (mm)	20	20	10	10
	Hole spacing (mm)	200	200	55	110
	Number of holes	2	2	2	2
Internal duct	Diameter (mm)	-	600	600	600
	Hole diameter (mm)	-	20	10	10
	Hole spacing (mm)	-	200	110	110
	Number of holes	-	2	4	4
Ratio of A_{OH} to A_{IH}		-	1	1	0.5

Table 2. Mesh design for grid independence test.

Scenario		**Coarse**	**Normal**	**Fine**
S0	Number of elements (million)	1.3	1.4	2.2
	Minimum element size	0.500	0.050	0.040
S1	Number of elements (million)	2.4	4.7	8.9
	Minimum element size	0.040	0.020	0.015
S2	Number of elements (million)	7.9	9.2	11.4
	Minimum element size	0.040	0.020	0.015
S3	Number of elements (million)	5.6	6.9	11.9
	Minimum element size	0.040	0.020	0.015

Table 3. Coefficient of variation for the mass flow rate and temperature at holes in S0–S3.

Scenario	CV for mass flow rate at holes (%)	CV for temperature at holes (%)
S0	6.5	1.2
S1	5.8	0.3
S2	6.2	0.3
S3	3.8	0.4